Developmental Biology

Mechanical forces pattern endocardial Notch activation via mTORC2-PKC pathway

Reviewed Preprint
v2 • January 16, 2025
Revised by authors

Reviewed Preprint
v1 • June 5, 2024

Yunfei Mu, Shijia Hu, Xiangyang Liu, Xin Tang, Jiayi Lin, Hongjun Shi

Fudan University, Shanghai, China • Key Laboratory of Growth Regulation and Translational Research of Zhejiang Province, School of Life Sciences, Westlake University, Hangzhou, China • Westlake Laboratory of Life Sciences and Biomedicine, Hangzhou, China • Institute of Basic Medical Sciences, Westlake Institute for Advanced Study, Hangzhou, China

eLife Assessment

Notch1 is expressed uniformly throughout the mouse endocardium during the initial stages of heart valve formation, yet it remains unclear how Notch signaling is activated specifically in the AVC region to induce valve formation. To answer this question, the authors used a combination of in vivo and ex vivo experiments in mice to demonstrate ligand-independent activation of Notch1 by circulation induced-mechanical stress and provide evidence for stimulation of a novel mechanotransduction pathway involving post-translational modification of mTORC2 and Protein Kinase C (PKC) upstream of Notch1. These findings represent an **important** advance in our understanding of valve formation and the conclusions are supported by **convincing** data.

https://doi.org/10.7554/eLife.97268.2.sa3

Abstract

Summary

Notch signaling has been identified as a key regulatory pathway in patterning the endocardium through activation of endothelial-to-mesenchymal transition (EMT) in the atrioventricular canal (AVC) and proximal outflow tract (OFT) region. However, the precise mechanism underlying Notch activation remains elusive. By transiently blocking the heartbeat of E9.5 mouse embryos, we found that Notch activation in the arterial endothelium was dependent on its ligand Dll4, whereas the reduced expression of Dll4 in the endocardium led to a ligand-depleted field, enabling Notch to be specifically activated in AVC and OFT by regional increased shear stress. The strong shear stress altered the membrane lipid microdomain structure of endocardial cells, which activated mTORC2 and PKC and promoted Notch1 cleavage even in the absence of strong ligand stimulation. These findings highlight the role of mechanical forces as a primary cue for endocardial patterning and provide insights into the mechanisms underlying congenital heart diseases of endocardial origin.

1. Introduction

The formation of the mammalian heart begins with a simple linear heart tube which undergoes complex morphogenic processes to ultimately reach the adult four-chamber configuration. In mice, the pattern of the adult heart becomes apparent at embryonic day (E) 9.5. At this stage, increased cell proliferation and sarcomeric development at the outer curvature of the primary heart tube lead to the formation of working chamber myocardium, while less proliferative and less differentiated myocardium at the inner curvature characterizes the outflow tract (OFT) and atrioventricular canal (AVC) [1], [2]. Between E9.5 and E10.5, endocardial cells in the OFT and AVC regions undergo extensive endothelial-to-mesenchymal transition (EMT), forming endocardial cushions. Further growth and remodeling of these endocardial cushions contribute to the septation of the OFT and cardiac chambers and give rise to cardiac valves [3]. Malformation of the endocardial cushions underlies the mechanism of the majority of human congenital heart defects (CHD).

Multiple interactive signal transduction pathways are involved in patterning valve versus chamber myocardium and regulating EMT. At E9.5, expression of BMP2 in the AVC and OFT myocardium [4], [5] directly activates TBX2 expression, which, in turn, activates TGFβ2 expression [6]. Both BMP2 and TGF-β2 enhance Snail1 expression and stimulate EMT [4], [7]. Notch signaling is also required for EMT. At E9.5, NICD (Notch1 intracellular domain) expression is the highest in endocardial cells of the AVC and OFT region, while in the ventricle, NICD is more restricted to the endocardium at the base of developing trabeculae [8],[9]. Notch, through the transcriptional factor CSL, directly activates Snail2 expression, leading to the repression of VE-cadherin expression [7], [10]. Genetic abrogation of Notch signaling blocks EMT in the AVC endocardium, whereas ectopic endocardial NICD expression leads to partial EMT of ventricular endocardial cells outside AVC [10], [11].

Despite the well-characterized role of Notch in endocardial patterning and EMT, little is known about the mechanism that specifically activates Notch in the areas of endocardium that undergo EMT. Among various Notch receptors and ligands, Notch1, Dll4, and Jag1 are expressed in the endocardium at the onset of EMT [10], [12]. Notch1 transcript appears to be uniformly expressed throughout the endocardium at E9.5, while Dll4 is most concentrated in the ventricular endocardium at the base of the trabeculae [9]. Jag1 is highly expressed throughout the myocardium, with only a few individual AVC endocardial cells positive for Jag1 [13], [14]. Conditional deletion of Dll4 in all endothelial cells results in the loss of classic EMT markers and complete absence of AVC cushions at E9.5 [13]. However, it remains unclear whether this impact on EMT is specifically due to the loss of Dll4-Notch signaling at cushion endocardium or a consequence of global circulatory failure resulting from vascular deformation in Dll4-deficient embryos. Therefore, the currently known expression pattern of Notch receptors and ligands does not fully explain the specific pattern of Notch activation in the endocardium.

Studies in zebrafish embryos have revealed the essential role of various mechanosensitive ion channels in modulating Notch1b receptor expression in the AVC endocardium in response to increased shear stress in this area [15]–[17]. However, as mentioned earlier, in the developing mouse endocardium at the onset of EMT, Notch1 is uniformly expressed throughout the endocardium despite restricted NICD in AVC and OFT endocardium. Thus, the equivalent mechanosensitive pathways controlling region-specific pattern of Notch activation, and hence EMT, in the mammalian endocardium are still unclear. To address this question, we transiently blocked the heartbeat of mouse embryos at E9.5 *in vivo* using the class III antiarrhythmic drug dofetilide, which selectively blocks the rapid component of the delayed rectifier K^+ current (I_{Kr}) in cardiomyocytes [18]. We found that Notch activation in the vascular endothelium is dependent on Dll4, whereas in the endocardium, the overall reduction of Dll4 expression creates a ligand-

depleted field that allows establishment of a specific Notch activation pattern in the AVC and OFT regions in response to increased shear stress. Strong shear stress in these valve-forming areas alters the membrane lipid microdomain structure of the endocardial cells, which then activates mTORC2 and PKC, promoting Notch1 cleavage even in the absence of strong ligand stimulation. The results uncovered a new mechanism whereby mechanical force serves as a primary cue for endocardial patterning in mammalian embryonic heart.

2. STAR methods

2.1. Reagents

A list of the reagents used in this study is provided in Table S1.

2.2. Animals

All mice used in this study were housed at a constant temperature (23°C) and humidity (~50%) with a 12-h light/dark cycle and ad libitum access to food and water. All animal experiments were performed in accordance with the protocol approved by the Westlake University Institutional Animal Care and Use Committee (approval # 21-007-SHJ). Noon of the day of vaginal plug detection was defined as embryonic day (E) 0.5. For dofetilide treatment, mice were gavaged at E9.5 with a single dose of dofetilide at 2 mg/kg dissolved in saline. For phorbol 12-myristate 13-acetate (PMA, 2 mg/kg) administration, mice were gavaged at E9.5 with a single dose of PMA dissolved in CMC-Na. Verapamil was given by intraperitoneal injection at E9.5. At the indicated date post-treatment, the dams were sacrificed by cervical dislocation, and the embryos were harvested for further analysis. All sources of our mouse lines are listed in Table S1. Knockout mice generated in-house are described and validated in Figure 3—Figure supplement 2E.

2.3. Fetal echocardiography

Ultrasound scanning was performed using the Vevo 300 high-frequency ultrasound machine (FUJI FILM Visual Sonics Inc., Canada). *In utero* echocardiography of fetal mice was conducted at E9.5. Transducer MX-550D had a central frequency of 40 MHz with axial and lateral resolutions both about 30 μm. The pregnant mice were sedated using 2% isoflurane and kept at 1% isoflurane to maintain body temperature at 35.5-37°C and heart rate at 400 to 500 beats per minute (bpm). Pulse-wave Doppler was used to measure velocity and time interval parameters to measure the blood flow velocity and time interval parameters of the fetal hearts. All fetuses were scanned twice in order and their *in utero* positions were noted. For embryos of $cTnT^{cre}$ x $Tnnt2^{flox/flox}$, after completing the Doppler ultrasound imaging, the embryos were dissected out with the recorded positions, and embryonic tissues were collected for genotype identification to correlate with the heart rate data. During the measurements, observers were blinded to the assigned groups. Analysis was performed with Vevo Lab 5.7.1.

2.4. Fetal heart morphology

Fetal hearts were imaged using the Zeiss Lightsheet Z.1 microscope. Embryos were harvested at E18.5, and hearts were dissected in phosphate-buffered saline (PBS), fixed overnight in a mixed solution of 10% neutral buffered formalin and 2.5% glutaraldehyde, then rinsed twice in PBS, and dehydrated in 50, 75 and 100% ethanol for 30 mins each at room temperature (RT). Samples were then transferred into a specially designed glass tube containing 100 μL of BABB solution (1:2 benzyl alcohol: benzyl benzoate) and incubated for 30 mins to clear the sample. The glass tube was mounted into the sample chamber which was filled with 87% glycerol (RI~1.45). Hearts were scanned from the apex to the great arteries for tissue autofluorescence using the 561 nm laser line and the detection optics 5x/0.16 (n=1.45). 3D reconstruction of the image stacks and morphological analyses were performed with Imaris 9.3 software.

2.5. *Ex vivo* embryo culture

Mouse embryos at E9.5 were carefully dissected in Hanks Buffer containing calcium and magnesium to remove decidua without damaging their yolk sacs and placentas. They were then cultured in 1 mL embryo culture medium (50% rat serum, 50% DMEM), pre-saturated with a gas mix of 95% O_2 and 5% CO_2 in a 5 mL volume glass tubes. Tubes were sealed and placed in an rotatory shaker maintained at 37 °C and 50 rpm. For pharmacological treatment, stauroporine (100 nM), wortmannin treatment (2 μM), dofetilide (0.2 ug/ml), or water-soluble cholesterol (1 mg/ml) was diluted in embryo culture medium to the desired concentrations.

2.6. Immunofluorescence and *in situ* hybridization

E9.5 and E10.5 wild embryos were dissected in PBS, fixed in 4% paraformaldehyde (PFA) overnight at 4 °C, dehydrated in ethanol series, cleared in xylene, and embedded in paraffin. Tissues were sectioned at 6 μm thickness. Paraffin sections were subjected to a 20 mins heat-induced antigen retrieval using a citric acid solution (pH 6). The sections were blocked with 5% normal donkey serum (NDS) in Tris-buffered saline with 1% Tween-20 (TBST) for 1 hour, followed by overnight incubation at 4°C with primary antibodies diluted in the blocking buffer. Bound primary antibodies were detected using fluorescently conjugated corresponding secondary antibodies. For detection of low-abundance targets such as NICD and phospho-PKC^{Ser660}, tyramide signal amplification (TSA) was applied. A list of the antibodies used in this study are provided in Table S1. Confocal microscopy images were captured on a Zeiss LSM 800 and image analysis was performed using Zen 2.3. Fluorescent intensity was calculated using ImageJ software.

To analyze NICD expression in E8.5, E9.5 mouse hearts, whole mouse embryos were fixed in 4% PFA at 4°C overnight. After blocking in 5% NDS, 0.5% Triton X-100 in TBS at 4°C overnight, samples were incubated at 4°C overnight with the primary NICD antibody diluted in blocking buffer (1:400). After washes, embryos were incubated with donkey anti rabbit HRP (1:500) 4°C overnight. Embryos were then washed and reacted with a tyramide-biotin solution at RT for 30 minutes. After that, samples were washed and incubated with Cy^{TM}3 streptavidin (1:500). Stained embryos were dehydrated in methanol, cleared in BABB and imaged by Zeiss LSM 800.

Whole mount in situ hybridization of *Dll4* were performed using the HCR probe set according to the manufacturer's instruction (Molecular Instruments, Los Angeles). Stained embryos were dehydrated in methanol, cleared in BABB and imaged by Zeiss LSM 800.

2.7 Scanning electron microscopy

E9.5 embryos are fixed with a solution containing 2% paraformaldehyde and 2.5% glutaraldehyde (pH 7.2) at 4°C overnight. The fixed embryos are then washed three times with 0.1M phosphate buffer (PB, pH 7.2–7.4) at 4°C for 10 minutes each. Subsequently, the samples are further fixed with 1% osmium tetroxide in 0.1M PB on ice for 1 hour. After fixation, they are rinsed three times with double-distilled water (ddH_2O) at room temperature for 15 minutes each. Dehydration is carried out at room temperature using a graded ethanol series: 30% ethanol for 10 minutes, 50% ethanol for 10 minutes, 70% ethanol for 10 minutes, 95% ethanol for 10 minutes, and absolute ethanol three times for 10 minutes each. Then the dehydrated samples are subjected to critical point drying. Samples were attached to a sample holder with double-sided carbon tape, and coated with a 10–15 nm thick metal film for SEM imaging.

2.8 Statistics

Difference in expression levels were tested using two-tailed t test. Two-sided Fisher's exact test was used to compare the heart defect rates between two groups. P value <0.05 was considered significant. All statistical analyses were performed in GraphPad Prism 8 software.

3. Results

3.1. Notch is strongly activated in the AVC and proximal OFT endocardium in spite of weak ligand expression at the onset of EMT

Although Notch1, Dll4, and Jag1 have been reported as the principal receptor and ligands expressed in the endocardium [12], [13], [19], the relationship between the Notch activity and its ligand expression in various parts of the E8.5-9.5 endocardium have not been examined in sufficient details. To investigate whether regional-specific Notch activation is due to differential receptor or ligand expression, we performed whole-mount *in situ* hybridization and immunofluorescence staining of Notch1, NICD, Dll4, and Jag1. Both *Dll4* transcripts and NICD were uniformly positive throughout all endothelial lining of the dorsal aorta and heart at E8.5 (Figure 1—Figure supplement 1A, Video S1, S3). However, at E9.5 when endocardial EMT starts, distinct patterns of NICD and Dll4 expression appeared (**Figure 1B** and Video S2, S4). Based on the expression pattern of NICD and Dll4, overall, the endocardium at E9.5 can be viewed as three distinct types as summarized in **Figure 1A**. Type I is Dll4-high and NICD-high, including the endocardium lining the distal OFT, the base of the trabeculae, the dorsal wall of the left atrium, and the right atrium. These endocardial cells normally do not undergo EMT. Type II is Dll4-low and NICD-high, including the AVC and proximal OFT endocardium. Endocardial cells in these regions undergo EMT to form endocardial cushion cells. Type III is Dll4-low and NICD-low, including the endocardium flanking the AVC and on the top of ventricular trabeculae (**Figure 1B** and Figure 1-Figure supplement 1C). Jag1 was highly expressed in the myocardium but expressed at a very low level in a small subset of the OFT and AVC endocardial cells (Figure 1—Figure supplement 1A), consistent with the previous report [13]. Vascular endothelium continued to express high levels of Dll4 and NICD uniformly, similar to type I endocardial cells. Dll4 protein staining pattern overlapped with the *Dll4* transcript and also agreed with VEGF receptor-2 (Flk1/KDR) protein expression throughout the cardiovascular endothelium at both E8.5 and E9.5 (Figure 1—Figure supplement 1B), consistent with the regulatory role of VEGF signaling in Dll4 expression [20]. Thus, the Dll4 and NICD expression patterns were disconnected in the type II endocardium at E9.5, suggesting the existence of additional mechanisms for Notch activation.

One previous study showed that endocardial EMT was dependent on Dll4 [13]. To further dissect the role of Dll4 in regional Notch activation, we conditionally deleted Dll4 in all endothelial cells using the $Tie2^{cre}$ line. At E9.5, *Dll4* conditional null AVC cushions were poorly cellularized, consistent with the previous finding. Furthermore, in most areas normally expressing high Dll4, i.e., vascular endothelium and aortic sac, NICD was completely abolished, whereas in the AVC, proximal OFT, and the base of the trabeculae, NICD was reduced but not completely absent (**Figure 1C**). As conditional deletion of Dll4 resulted in embryos with severely disorganized vasculature (**Figure 1C**), we cannot rule out the possibility that the reduced NICD in the AVC might not be simply due to Dll4 deletion, but rather affected by circulatory failure. These findings indicate that vascular endothelium is dependent on Dll4 for Notch activation, whereas in the endocardium, additional factors are required to pattern Notch activation in the proximal OFT and AVC.

3.2. Notch activation in cushion endocardium is dependent on blood flow

Work in the past on zebrafish embryos showed that cardiac contraction activates endocardial Notch signaling[21]. To test if Notch activation is regulated by blood flow in the developing mouse heart, pregnant mice were gavaged with a single dose of dofetilide at 2mg/kg at E9.5. The embryos were then either harvested immediately after the treatment or allowed to develop until E18.5

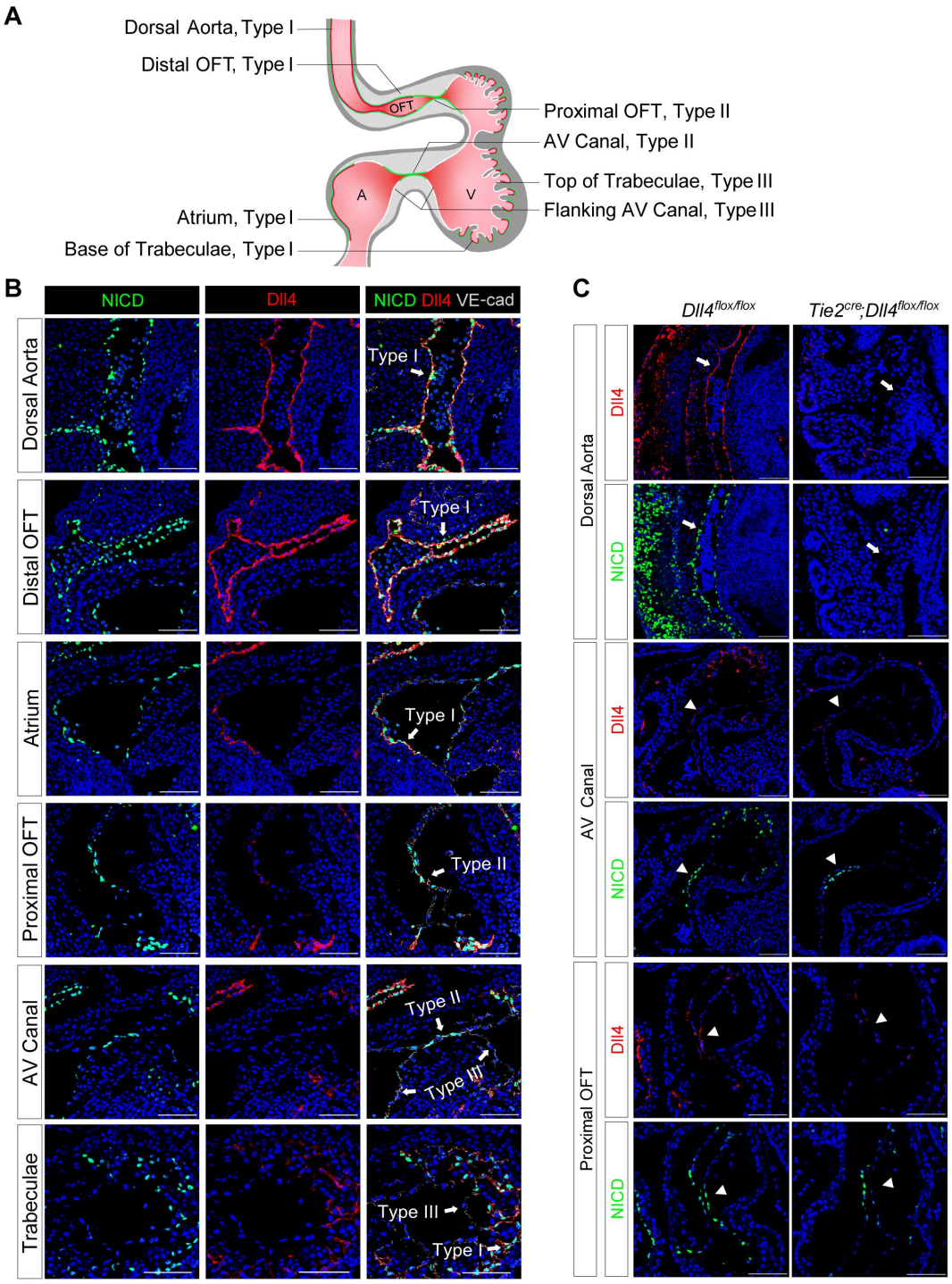

Figure 1

Endocardium and vascular endothelium of dorsal aorta showed different patterns of Notch1 activation and Dll4 ligand expression.

A, Schematic representation of 3 types of endothelial cells and their corresponding localizations. **B,** Type I cells are NICD-high and Dll4-high. Type II cells are NICD-high and Dll4-low. Type III cells are NICD-low and Dll4-low. Scale bars, 100 μm. (*n* = 3 embryos) **C,** Representative images showing Dll4 protein and NICD in wild-type and endothelial-specific *Dll4*-deleted (*Tie2*^{cre};*Dll4*$^{flox/flox}$) E9.5 mouse hearts. Scale bars, 100 μm. (wild-type: *n* = 3 embryos; *Tie2*^{cre};*Dll4*$^{flox/flox}$: *n* = 3 embryos)

when cardiac morphology was assessed (Figure 2—Figure supplement 1A). Dofetilide caused an immediate stop of blood flow in the embryos, as observed by doppler ultrasound from 1 h through to 3 h, which completely recovered at 5 h post-treatment (**Figure 2A** and Video S5, S6). Three hours cessation of blood flow caused a complete loss of NICD without affecting total Notch1 receptor protein in the proximal OFT and AVC endocardium. The loss of NICD was completely recovered at 5 h post-treatment, in line with the dynamics of the heart rate changes (**Figure 2B**), while no significant changes in the expressions of Dll4 and Jag1 were noted in AVC endocardium after dofetilide treatment (**Figure 2B**). Pro-EMT markers phospho-Smad1/5, Sox9 and Twist1 were downregulated in the AVC endocardium after cardiac arrest (**Figure 2B**). Interestingly, NICD in the dorsal aorta was resistant to the cessation of flow (Figure 2—Figure supplement 1B). Consistent with the inhibition of EMT, transient cessation of blood flow resulted in hypoplastic AVC endocardial cushions 5 hours after treatment (Figure 2—Figure supplement 1C) and more pronounced cushion hypoplasia one day after treatment (**Figure 2C**), and various heart defects (**Figure 2D** and Figure 2—Figure supplement 1D) in 40% of embryos: ventricular septal defects (VSD), bicuspid semilunar valve, atrioventricular valve defects, and conotruncal defects, consistent with malformation of endocardial cushions.

To rule out the possible direct effect of dofetilide on endocardial cells independent of flow, we conditionally deleted *Tnnt2* in the embryonic myocardium, which caused bradycardia in the E9.5 embryos and lethality at E10.5 (Video S7). Similar to the effect of dofetilide, reducing blood flow rate by genetic means also caused a significant reduction of NICD in the cushion endocardium at E9.5 (Figure 2—Figure supplement 2A). Furthermore, block of heart beat by *ex vivo* blebbistatin treatment, an inhibitor for non-muscle myosin II ATPase, also prevented Notch cleavage in the cushion endocardium at E9.5 (Figure 2—Figure supplement 2B). To rule out the possible effect of hypoxia on Notch activation, we depleted embryonic erythrocytes by crossing $Epor^{cre}$ with ROSA-DTA mouse line, which resulted in widespread hypoxia without interfering embryonic heartbeat, yet NICD was normal in the AVC endocardium (Figure 2—Figure supplement 2C). We also cultured E9.5 embryos in a medium saturated with 95% O_2 in the presence of dofetilide for 3 h. High levels of O_2 eliminated HIF-1α nuclear staining induced by cardiac arrest, while NICD was still absent in the AVC endocardium (Figure 2—Figure supplement 2D). Thus, all subsequent *ex vivo* embryo culture experiments were performed in 95% O_2 to minimize the effect of hypoxia on Notch activation. Collectively, these results indicate that Notch activation and EMT in the cushion endocardium are dependent on the mechanical stimulation from blood flow.

3.3. Flow-responsive mTORC2-PKCε activity is required for Notch activation in the cushion endocardium

Given the fast response of NICD to flow cessation, we suspect a change in post-translational modification, such as a phosphorylation event, that might mediate the effect. PKC, AKT, and ERK have all been reported to have their phosphorylation status altered in response to fluid shear stress in cultured endothelial cells [22]. In addition, *in vitro* shear stress-induced Notch activation can be blocked by inhibitors of PKC, AKT, and ERK [23]. Therefore, we examined the phosphorylation status of these three signaling molecules in the endocardium before and after dofetilide treatment. Both pPKC (βII^{Ser660}) and $pAKT^{Ser473}$ were restricted to the cushion endocardium and the base of the trabeculae in control embryos and were almost completely lost as quickly as 1 h after treatment and then both recovered at 5 h after treatment. Both pPKC and pAKT were not detectable in dorsal aorta endothelium (**Figure 3A** and Figure 3—Figure supplement 1A). Their response rate in cushion endocardium was faster than NICD, whose maximum inhibition occurred at 3 h post-treatment (**Figure 2C**). pERK was not detectable in the cushion endocardium (Figure 3—Figure supplement 1B). Inhibition of AKT phosphorylation in cultured E9.5 embryos by wortmannin did not inhibit Notch activation (Figure 3—Figure supplement 1C), whereas inhibition of PKC activity by staurosporine treatment blocked Notch activation (**Figure 3B**).

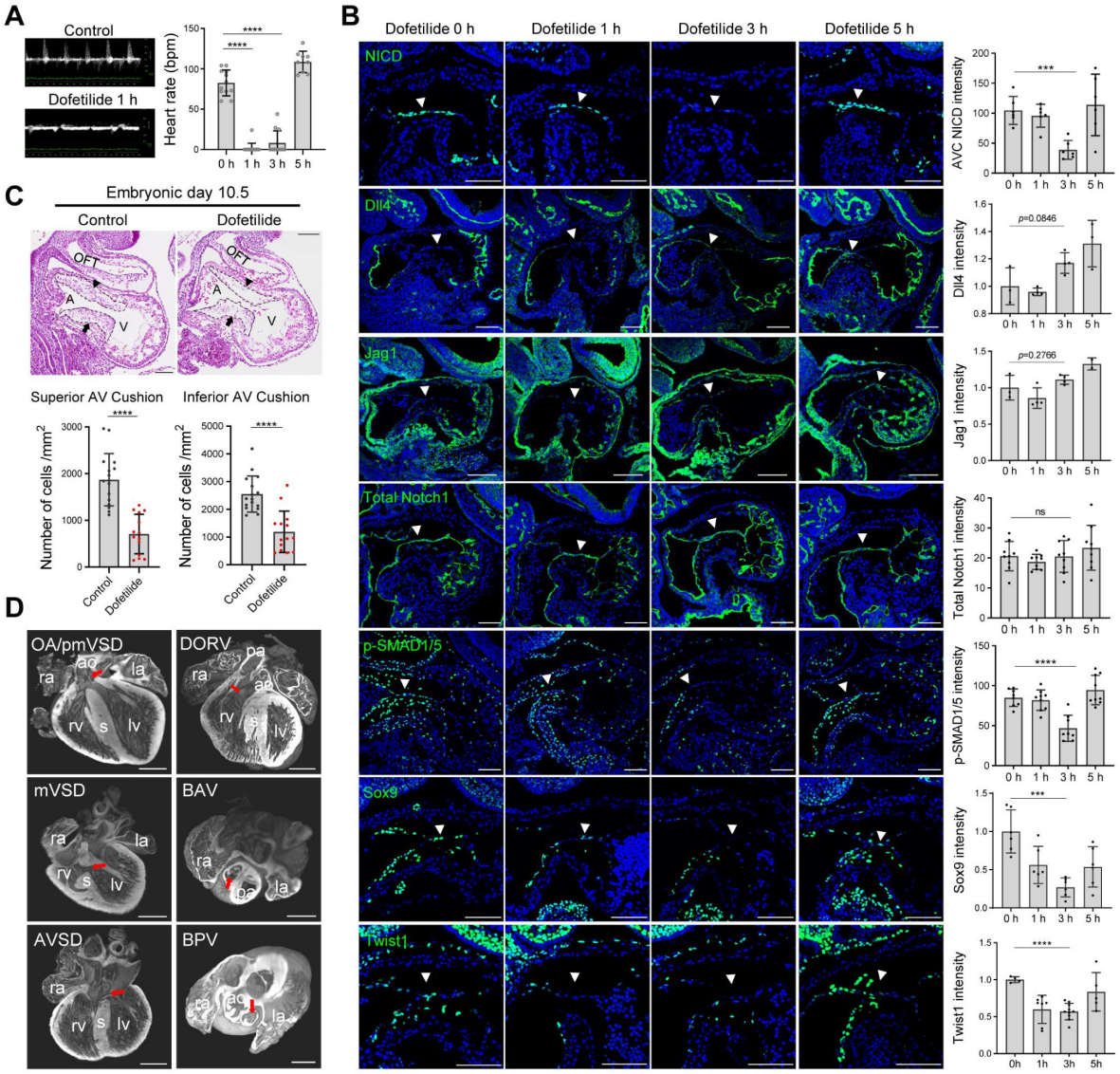

Figure 2

Notch activation in cushion endocardium is dependent on blood flow.

A, Echocardiography of control and dofetilide treated embryos. (0 h: *n* = 12; 1 h: *n* = 15; 3 h: *n* = 12; 5 h: *n* = 9). **B,** Expression of NICD, Dll4, Jag1, total Notch1, p-SMAD1/5 and Sox9, Twist1 in the E9.5 dorsal aorta endothelium (arrow) and endocardium (arrowhead). **C,** Sagittal E10.5 hematoxylin-eosin stained sections demonstrated hypocellularity in both superior (arrowhead) and inferior AV cushion (arrow) caused by dofetilide treatment. Quantification of mesenchymal cell density in superior (below left) and inferior (below right) AV cushion (Control: *n* = 16 embryos; Dofetilide: *n* = 14 embryos). OFT, outflow tract; A, atrium; V, ventricle. **D,** Representative heart defects induced by maternal dofetilide treatment. pmVSD, perimembranous ventricular septal defect; DORV, double-outlet right ventricle; mVSD, muscular VSD; OA, overriding aorta; BAV, bicuspid aortic valve; AVSD, atrioventricular septal defect; BPV, bicuspid pulmonary valve; ra, right atrium; la, left atrium; ao, aorta; rv, right ventricle; lv, left ventricle; s, interventricular septum; pa, pulmonary artery. Scale bars, 100 μm (**B, C**), 500 μm (**D**). (*n* > 3 for every group and each condition)

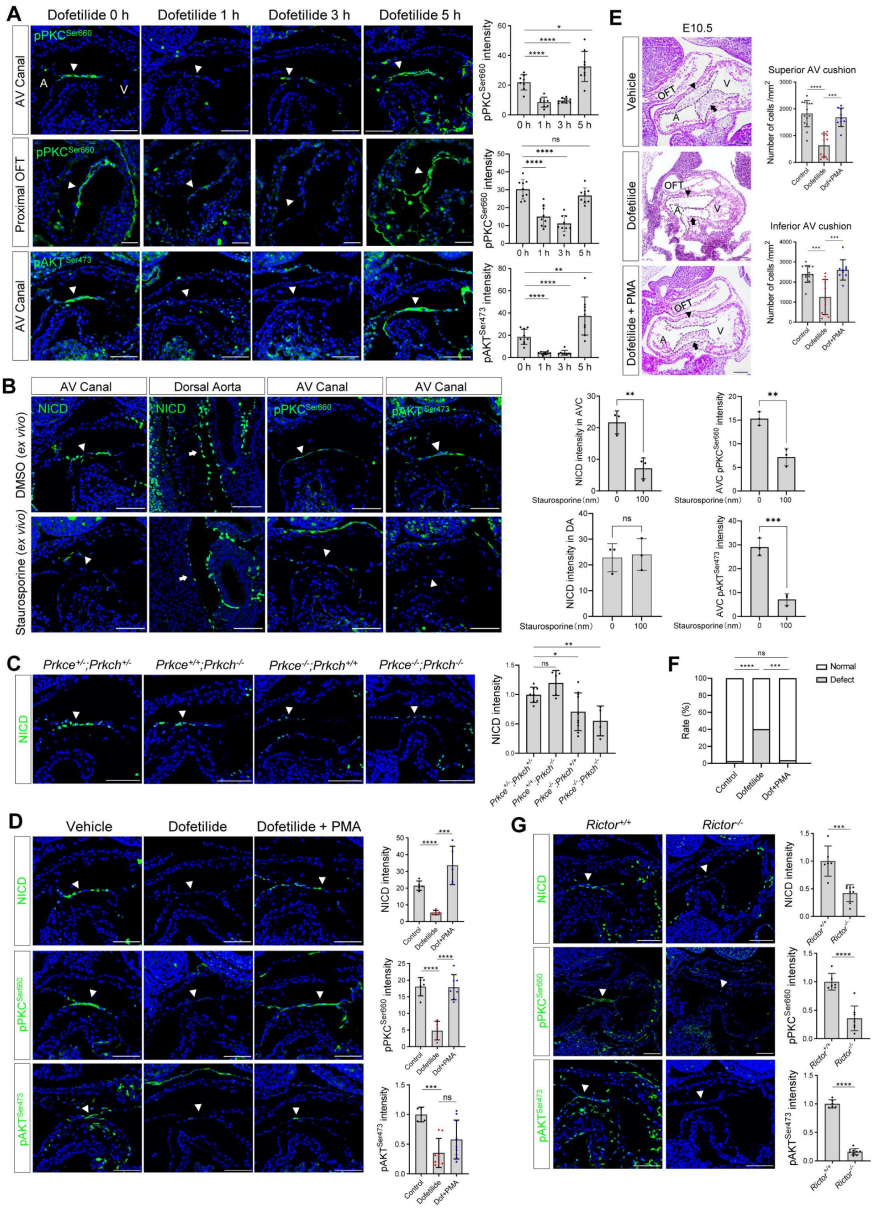

Figure 3

Flow-responsive mTORC2-PKCε activity is required for Notch activation in the cushion endocardium.

A, Phospho-PKC^{Ser660} and phospho-AKT^{Ser473} levels in the atrioventricular (AV) canal endocardium and proximal OFT endocardium (arrowhead) after dofetilide treatment. Each point in the quantification chart represents one embryo. **B,** NICD, pPKC and pAKT expression in cultured E9.5 heart in response to *ex vivo* staurosporine treatment (100 nM). Each point in the quantification chart represents one embryo. **C,** NICD expression in AV canal endocardium in wild-type, *Prkce* and *Prkch* single knockout and double knockout embryos. Each point in the quantification chart represents one embryo. **D,** NICD, p-PKC^{Ser660} and p-AKT^{Ser473} staining in AVC endocardium (arrowhead) after dofetilide treatment and after rescue by PMA. **E,** Sagittal E10.5 HE staining sections demonstrates acellularized superior (arrowhead) and inferior AV cushion (arrow) caused by dofetilide which were rescued by in PMA treatment (2 mg/kg). OFT, outflow tract; A, atrium; V, ventricle. Mesenchymal cell density was quantitated in superior and inferior AV cushion (Control: *n* = 14 embryos; Dofetilide: *n* = 11 embryos; Dofetilide + PMA: *n* = 9 embryos). **F,** Heart defect rate caused by maternal dofetilide and PMA treatment (Control: *n* = 37; Dofetilide: *n* = 62; Dofetilide + PMA: *n* = 27). **G,** NICD, phospho-PKC^{Ser660}, and phospho-AKT^{Ser473} in AV canal endocardium (arrowhead) in wild-type and *Rictor* null mice (*Rictor*$^{+/+}$: *n* = 6; *Rictor*$^{-/-}$: *n* = 8). Scale bars, 100 μm.

To further confirm the role of PKC in regulating Notch, we individually knocked out *Prkce* and *Prkch* (Figure 3—Figure supplement 2C). Among all PKC family members, these two isozymes are most highly expressed in the endocardium based on RNAseq analysis of E9.5 embryos' endocardial and vascular endothelial cells (Figure 3—Figure supplement 2A). $Prkch^{KO}$ did not affect Notch activation or produce any phenotype. $Prkce^{KO}$ caused a slight but significant reduction of NICD in the cushion endocardium at E9.5 and caused 25% heart defects at E18.5. *Prkce/Prkch* double knockout resulted in a further loss of NICD at E9.5, leading to pericardial effusion and complete lethality at E10.5. (**Figure 3C** and Figure 3— Figure supplement 2E). No pericardial effusion or heart beating abnormalities was noted at E9.5 in these mutant embryos (Figure 3—Figure supplement 2D), suggesting a direct action of PKCs on Notch signaling, rather than indirect action through affecting blood flow. Treatment of pregnant mice at E9.5 with a potent PKC activator, phorbol 12-myristate 13-acetate (PMA), almost completely rescued dofetilide-induced loss of NICD, pPKC, cushion hypoplasia, and cardiac defects (**Figure 3D**-**3F**). The restricted activation of NICD in AVC region by PMA treatment is consistent with the restricted expression of PKCε and PKCη in the AVC endocardium (Figure 3-supplement figure 2B). Thus, PKC activity is both necessary and sufficient for Notch activation in the cushion endocardium.

Both PKC and AKT belong to the AGC kinase family and both have a conserved hydrophobic motif at the C-terminal tail of the catalytic domain, whose phosphorylation is dependent on mTORC2 and is required for kinase activity [24]. Therefore, the observed inhibition of hydrophobic motif phosphorylation of PKC and AKT indicates impairment of the common upstream activator mTORC2. We conditionally deleted one of the essential mTORC2 components, Rictor[25], in the endothelial cells (Figure 3—Figure supplement 2C). As expected, ablation of mTORC2 completely blocked hydrophobic motif phosphorylation of both PKC and AKT and consequently led to significant decrease of NICD in the cushion endocardium (**Figure 3G**). Thus, blood flow activates Notch in the cushion endocardium via mTORC2-PKC signaling pathway.

3.4. Shear stress-induced alteration of membrane lipid microstructure activates mTORC2-PKC-Notch signaling pathway

In cultured mammalian endothelial cells, fluid shear stress (FSS) increases the number of cell surface caveolae, a specialized membrane microdomain enriched for cholesterol and sphingolipids; sequestration of cholesterol inhibits shear-dependent activation of ERK [26]. Thus, we tried to manipulate the membrane lipid microdomain by treating the cultured E9.5 embryos with cholesterol. Staining of Caveolin-1, the major component of caveolae, showed that Caveolin-1 was normally expressed on the cell surface of the AVC endocardial cells including the luminal surface and the lateral cell adhesion sites. However, in area with low shear stress such as dorsal aorta endothelium, atrial, and ventricular endocardium downstream of AVC, Caveolin-1 was mainly restricted to the lateral cell adhesion sites and absent on the luminal surface. *Ex vivo* dofetilide treatment caused retraction of Caveolin-1 from the luminal surface to the lateral cell adhesion sites in the AVC endocardial cells, while co-treatment with cholesterol rescued the presence of Caveolin-1 to the luminal surface of AVC endocardial cell in the presence of dofetilide (**Figure 4A**). In addition, scanning electron microscopy on E9.5 AV canal endocardium showed numerous membrane invaginations on the luminal surface of the endocardial cells. The size of the invaginations ranged from 50 to 100 nm, consistent with the reported size of caveolae. Dofetilide significantly reduced the number of membrane invaginations, which recovered after restore of blood flow at 5 hours post dofetilide treatment (Figure 4—Figure supplement 1A). The reduction of membrane invaginations at 3 hours post ex vivo dofetilide treatment could be rescued by co-treatment of cholesterol (**Figure 4B**). The loss of NICD, $pPKC^{Ser660}$, and $pAKT^{Ser473}$ caused by dofetilide could all be rescued by pretreatment with cholesterol, indicating reactivation of mTORC2 (**Figure 4C**). These rescuing effects of cholesterol disappeared in the *Rictor* KO embryos (**Figure 4C**), suggesting mTORC2 was intermediate signaling molecules linking membrane lipid microstructure and Notch activation.

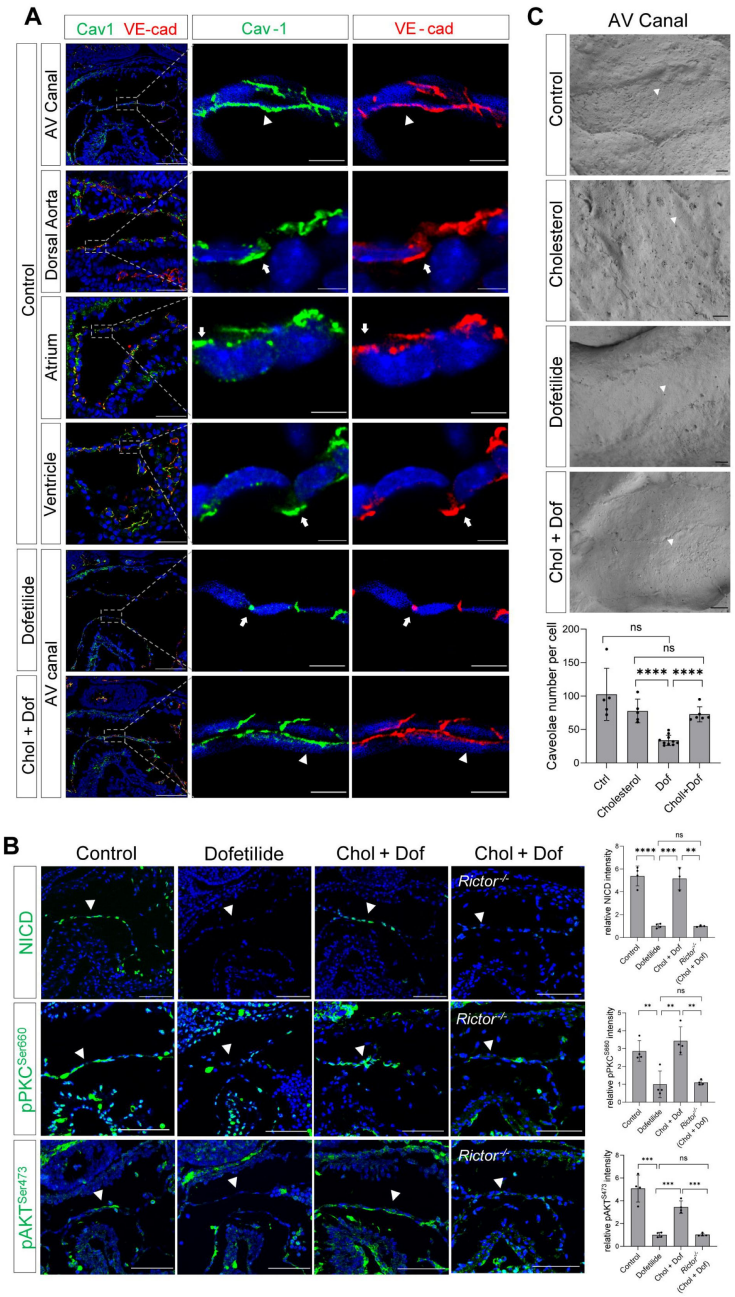

Figure 4

Shear stress-induced alteration of membrane lipid microstructure activated mTORC2-PKC-Notch signaling pathway.

A, Caveolin-1 and VE-cadherin expression in mouse E9.5 AV canal, dorsal aorta, atrium and ventricle endocardium, demonstrating luminal (arrowhead) and lateral (arrow) surface localization. *Ex vivo* dofetilide treatment (0.2 μg/ml) of cultured E9.5 embryos for 3 h caused retraction of Caveolin-1 and VE-cadherin from luminal surface of the AVC endocardial cells to the lateral cell adhesion sites which could be rescued by co-treatment with cholesterol (1 mg/ml). **B,** Representative images and quantifications of scanning electron microscopy on E 9.5 embryonic heart AV canal endocardial cells at their luminal surfaces, with caveolae structure presentively pointed by arrowhead. Each point in the quantification chart represents one embryo. **C,** Loss of NICD, phospho-PKC^{Ser660}, and phospho-AKT^{Ser473} in AVC endocardium (arrowhead) by *ex vivo* dofetilide treatment could be rescued by cholesterol. The rescue failed in *Rictor* null hearts. Each point in the quantification chart represents one embryo.Scale bars, 100 μm (**A, C**). Scale bars, 10 μm (**A**, zoom-in), 1 μm (**B**).

3.5. Pharmacogenetic interaction in etiology of congenital heart defects

Gene-environmental interactions are believed to underlie the complex etiology of many congenital heart diseases. With the mechanosensitive nature of Notch in mind, we speculated that reducing the gene dosage of Notch1 may interact with agents that disrupt normal hemodynamic stimulations to the endocardium and synergistically causes heart defects. To test this, we crossed Notch1 heterozygous null male (FVB) with wildtype female mice, and treated the pregnant mice with a lower dose of dofetilide (1.8 mg/kg) at E9.5. In addition, we tested another drug verapamil, a commonly used FDA-approved L-type calcium channel blocker for treatment of high blood pressure, heart arrhythmias, and angina[27], in FVB background. A single dose of maternal verapamil treatment at E9.5 significantly decreased embryonic heart rate (**Figure 5E**). Neither Notch1 heterozygosity alone, nor drug treatment alone at the applied dosage produced any notable heart defects. However, the combination of Notch1 mutation and drug exposure of either dofetilide or verapamil resulted over 50% of fetuses having various heart defects of endocardial origin (**Figure 5A-D**).

4. Discussion

In this study, we identified fluid shear stress as the primary activator of Notch signaling in the area of AVC and OFT of the mouse looping heart tube. Strong fluid shear stress in the AVC and OFT enhances PKC phosphorylation by mTORC2 possibly by maintaining a particular membrane microstructure. Activated PKC then augments Notch cleavage under the minimal ligand stimulation, resulting Notch activation and EMT specifically in areas of valve primordium characteristic of narrow internal diameter and high shear stress. These findings are directly relevant for endocardial patterning. Notch activity is known to be essential for establishing OFT and AVC endocardial cell identity capable of EMT [10], [11]. Activation of Notch in the AVC endocardium is presumed to be mainly driven by the Dll4 ligand because Dll4 has been demonstrated to be expressed in the AVC endocardial cells and endothelial-specific knockout of *Dll4* produced acellularized AV cushions [13]. However, careful examination of the immunostaining pattern revealed that NICD, VEGFR2 and Dll4 were initially expressed with equal levels throughout cardiovascular endothelium at E8.5 prior to endocardial EMT, but at E9.5 with the onset of EMT, endocardial VEGFR2 and Dll4 were markedly reduced and NICD becomes restricted to endocardium overlaying the merging OFT and AVC cushions, implying a transition of the main driver of Notch activation from the pan-endothelial VEGFR2-Dll4 stimulation at E8.5 to the regionally restricted shear force stimulation at E9.5.

We therefore propose the following working model as how mechanical cues guide Notch activation during endocardial patterning. Following gastrulation, high level of VEGF-VEGFR2 signaling in mesodermal tissues initiates Dll4 expression which activates Notch and drives arterial endothelium and endocardium differentiation and proliferation. At E9.5 when endocardial EMT starts, VEGF signaling must dampen due to its suppressive function on EMT [28], [29]. One way to lower VEGF signaling in the endocardium is through downregulating VEGFR2 expression. Consequently, Dll4 expression also decreases, rendering Notch less active in the endocardium compared to the vascular endothelium. In the meantime, cardiac ballooning on both sides of the AVC expands the myocardial chambers and widen the endocardial internal diameter, leaving only the endocardium of the OFT and AVC endocardial cushion region closely attached. Narrow blood passage way creates strong shear stress to stimulate Notch cleavage only in these narrow areas of future cardiac septation and valve formation. Thus, in the developing mouse hearts: (1) VEGF signaling is reduced to permit endocardial EMT; (2) Dll4 expression is reduced to prevent

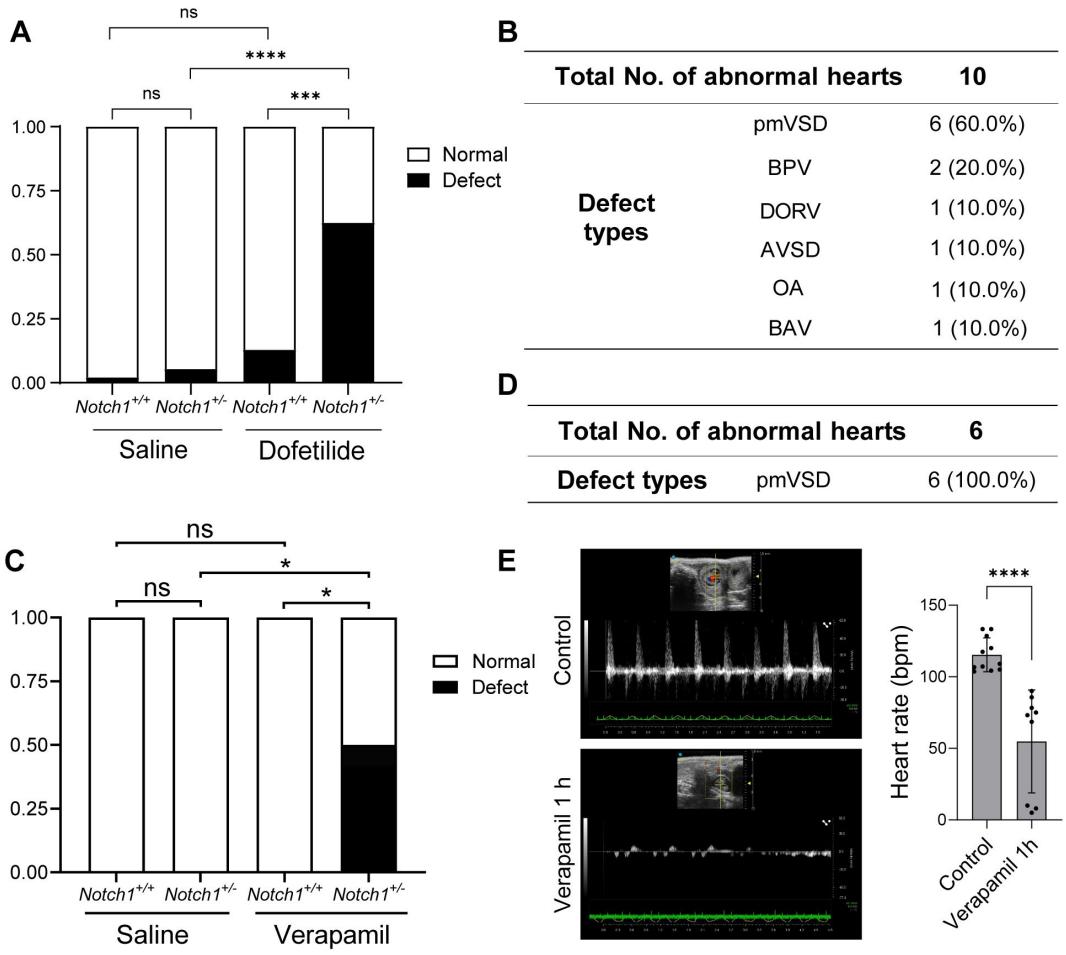

Figure 5

Pharmacogenetic interaction causing heart defects.

A, Heart defect rate significantly increased in Notch1 heterozygous embryos treated with dofetilide (1.8 mg/kg) at E9.5. (Saline *Notch1*$^{+/+}$: *n* = 48, Saline *Notch1*$^{+/-}$: *n* = 37, Dofetilide *Notch1*$^{+/+}$: *n* = 31, Dofetilide *Notch1*$^{+/-}$: *n* = 16). **B,** Types of heart defects in the dofetilide and *Notch1*$^{+/-}$ combined group. **C,** Heart defect rate significantly increased in Notch1 heterozygous embryos treated with Verapamil (15 mg/kg) at E9.5. (Saline *Notch1*$^{+/+}$: *n* = 18, Saline *Notch1*$^{+/-}$: *n* = 9, Verapamil *Notch1*$^{+/+}$: *n* = 8, Verapamil *Notch1*$^{+/-}$: *n* = 12). **D,** Types of heart defects in the verapamil combined with *Notch1*$^{+/-}$ group. **E,** Representative echocardiography and quantifications of heartbeat in control and verapamil treated E 9.5 embryos. Each point in the quantification chart represents one embryo.

widespread endocardial Notch activation and make endocardium sensitive to flow; (3) a proper cushion size and shape is maintained by limiting the flanking endocardium to undergo EMT despite physically close to the field of BMP2 derived from of AVC myocardium (**Figure 6**).

Studies in zebrafish identified several cation channels including Trpv4, Trpp2, Piezo1, Piezo2 and P2X that contribute to mechanosensing in the developing endocardium [15, 17, 30]. Blood flow in the looping mammalian heart is predominantly unidirectional whereas early zebrafish embryonic heart displays oscillatory flow pattern [17]. Mammalian embryonic endocardium undergoes extensive EMT to form valve primordia while zebrafish atrioventricular valve primordia is formed via partial EMT and the collective cell migration of endocardial cells into the cardiac jelly followed by tissue sheet delamination[15, 31, 32]. It is thus possible that mammalian hearts may evolve additional mechanisms to guide endocardial patterning and development. Our data support a model that membrane lipid microdomain acts as a shear stress sensor and transduces the mechanical cue to activate intracellular mTORC2-PKC-Notch signaling pathway in the developing endocardium. Shear stress has been shown to upregulate the number of caveolae in cultured endocardial cells [26]. Flow induced AKT phosphorylation is dependent on Caveolin-1 [33]. Both PKCα and PKCε interact with Caveolin-1 and bind with caveolae membranes [34, 35]. In neuronal cells or neural tissues, accumulation of psychosine in the plasma membrane disrupted lipid rafts, blocked recruitment of mTORC2 and PKC to the lipid raft, and inhibited AKT and PKC activation [36, 37]. In line with these previous findings, we demonstrated that high level of shear stress in the AVC and OFT is required for caveolin localization to the luminal surface of the endocardial cell membrane, and this membrane lipid microstructure is both necessary and sufficient for mTORC2-PKC-Notch pathway activation. The mechanism by which shear stress and cholesterol increases caveolae is unknown. In a previous study, shear stress exposure for a few minutes rapidly decreases the lipid order and increase the fluidity of the plasma membranes which appears to contradict our findings [38]. However, membrane lipid compositions are highly dynamic and regulated. It is possible that acute shear stress and its associated kinetic energy may initially decrease membrane lipid order, but long-term shear may evoke cellular feedback mechanisms to increase lipid order and enhance membrane rigidity. As cholesterol is an integral component of lipid raft and caveolae, it is likely that enrichment of cholesterol to the plasma membrane by exogenous supplementation might alter the membrane structure to make the lipid raft structure less dependent on sheer stress. It is noteworthy that the methodology used to alter blood flow in this study inevitably affects myocardial contraction. Thus, further work to uncouple changes in shear stress and myocardial mechanical properties, with the aid of theoretical modeling or using mouse heart valve explants, is needed to fully characterize the effect of shear stress on mouse endocardial development.

The positive regulation of Notch activation by PKC has been reported in a number of *in vitro* systems. Studies in $CD4^+$ T cells revealed that Notch is activated within hours of TCR stimulation independent of Notch ligands, and PKC activity is both sufficient and necessary for the ligand independent Notch activation [39]. The exact mechanism by which PKC regulate Notch processing is not known, and in need of further investigation in the future.

The vast majority of congenital heart diseases do not have a genetic explanation and are considered to have a multifactorial origin. Studies conducted on various model organisms such as chick and zebrafish have demonstrated that alterations in blood flow during early stages of heart development can lead to heart malformation [40]. Similarly, human studies have shown that fetal bradycardia or abnormal flow patterns in the Ductus Venosus during the first trimester of pregnancy are associated with an increased risk of CHD [41, 42]. Our research findings suggest that abnormal heart contraction or flow patterns, resulting from genetic mutations or the use of certain drugs during early heart development, may interact with genetic pathways involved in mechanosensing and endocardial EMT. These interactions could contribute to the complex etiology of congenital heart disease.

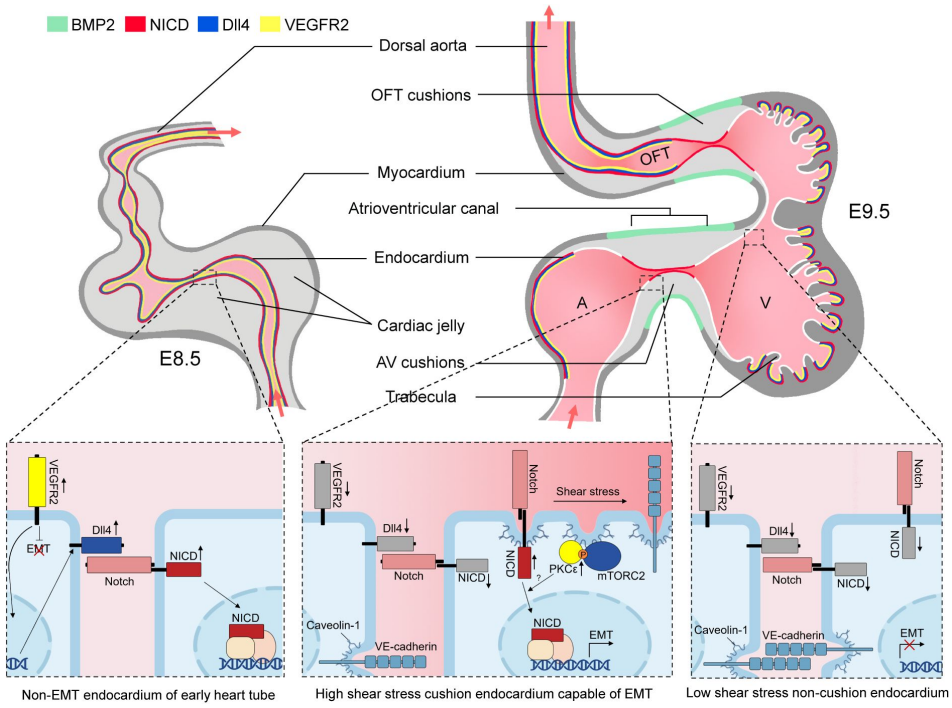

Figure 6.

Working model of the establishment of Notch activation pattern by mechanical cues.

The establishment of Notch activation pattern by mechanical cues involves a series of events in the developing heart tube. At E8.5, the arterial endothelium and non-EMT endocardium exhibit low shear stress, high VEGF, Dll4, and Notch signaling. One day later, the endocardium undergoes patterning and becomes capable of epithelial-to-mesenchymal transition (EMT) only in the AVC and proximal OFT regions. This patterning is achieved through restricted expression of BMP2 and NICD in these specific areas. EMT requires the downregulation of VEGF signaling by the endocardium, enabling EMT to occur. Additionally, Dll4 is downregulated in endocardium to prevent widespread Notch activation. Simultaneously, the high shear stress present in the AVC and proximal OFT regions leads to increased membrane lipid order, which activates the mTORC2-PKC-Notch pathway and promotes EMT. On the other hand, regions flanking these valve-forming areas experience lower shear stress, resulting in inactive Notch signaling and an inability to undergo EMT.

Acknowledgements

The authors are grateful to Dr. Xu Li of Westlake University for valuable suggestions regarding Notch experiments. We thank Dr. Zhen Zhang from Shanghai Jiao Tong University, Dr. Bing Zhang, Dr. Jiemin Jia, Dr. Shang Cai from Westlake University and Dr Hui Zhang from Shanghai Tech University for sharing mouse lines. We thank the Microscopy Core Facility of Westlake University for assistance and advice. We thank the Westlake Animal Facility and Youshi Chen for mouse breeding and husbandry. We thank Jianfeng Wang for assistance in *ex vivo* culture. This work was supported by Natural Science Foundation of Zhejiang Province of China (LZ19H040001) and Westlake Education Foundation.

Additional information

Author contributions

H.S. raised hypothesis, designed experiments, interpreted data and drafted the work. Y.M., and S.H. conducted the main body of the experiments, including mouse crosses and treatment, embryo harvest, staining and data analysis. X.L. made contributions by optimizing light sheet microscopy and performed work related to heart phenotyping. S.H. participated in manuscript drafting. X.T. characterized the change of membrane lipid structure induced by flow. J.L. assisted in the performances of echocardiography for both pregnant and fetal mice.

Additional files

Figure 1—figure supplement 1. *Notch is strongly activated in the AVC and proximal OFT endocardium despite weak ligand expression at the onset of EMT.**A,** Representative images of NICD (green) whole mount immunofluorescence, Dll4 (red) whole mount in situ hybridization, and Jag1 (yellow) immunofluorescence of E8.5 and E9.5 mouse heart. Arrows indicate arterial endothelium and arrowheads indicate endocardium. **B,** Representative images demonstrating VEGFR2 (Green) and Dll4 (red) protein expression in E8.5 and E9.5 mouse artery (arrowhead) and endocardium (arrow). **C,** Quantification of NICD and Dll4 immunofluorescence intensity within the area of each 3 types of endothelial cells.*

Figure 2–figure supplement 1. *A, Schematic diagram of the experimental design. **B,** Representative figures and statistics of NICD expression in dorsal aorta and POFT after dofetilide treatment. **C,** HE staining of E9.5 embryonic hearts and the quantifications of superior and inferior AV cushion cell density in control group and 5 hours after dofetilide treatment. (Control: n = 7 embryos; Dofetilide: n = 6 embryos) **D,** Heart defects induced by maternal dofetilide treatment. (0 mg/kg: n = 37; 2.0 mg/kg: n =117). pmVSD, perimembranous ventricular septal defect; DORV, double-outlet right ventricle; mVSD, muscular VSD; OA, overriding aorta; BAV, bicuspid aortic valve; AVSD, atrioventricular septal defect; BPV, bicuspid pulmonary valve.*

Figure 2–figure supplement 2. *A, Representative images of NICD in myocardial-specific cardiac troponin T knockout mouse heart. **B,** Representative images of NICD expression in AV canal, proximal OFT and dorsal aorta after blebbistatin treatment (5 μM) for 3 h. **C,** HIF-1α and NICD in red blood cell depleted E9.5 mouse hearts. **D,** Representative images of HIF-1α and NICD in E9.5 control, dofetilide-treated, and hyperoxia-treated mouse hearts. Arrow: dorsal aorta endothelium. Arrowhead: endocardium. Scale bars, 100 μm.*

Figure 3–figure supplement 1. *A, pPKC^{Ser660} in E9.5 mouse dorsal aorta, and pAKT^{Ser473} in E9.5 dorsal aorta endothelium.* ***B,*** *pERK1/2 was not detectable in AV canal endocardium.* ***C,*** *NICD in cultured E9.5 heart in response to ex vivo wortmannin treatment (2 μM).*

Figure 3–figure supplement 2. *A, Counts of conventional and novel PKC isoforms assessed by bulk RNA-seq of E9.5 embryonic endocardial cells. (n =4)* ***B,*** *Immunofluorescence staining of PKCε and PKCη in E9.5 embryonic hearts.* ***C,*** *Prkch, Prkce and Rictor knockout mice strategies and western blot or immunofluorescence confirmation of KO.* ***D,*** *Echocardiography of heterozygous Prkch, Prkce knockouts.* ***E,*** *Counts of abnormal hearts of the descendants of Prkch, Prkce double heterozygous intercrosses at E18.5. Arrow: dorsal aorta endothelium. Arrowhead: endocardium. Scale bars, 100 μm.*

Figure 4–figure supplement 1. *A, Scanning electron microscopy of E9.5 embryonic heart in AV canal endocardial cells at their luminal surfaces after dofetilide treatment at 3 hours and 5 hours, with caveolae structure presentively pointed by arrowhead. Caveolae density was quantified. Each group has 4 embryos.*

Supplement table 1. *Materials and Reagents.*

References

1. Moorman AF, Christoffels VM (2003) **Cardiac chamber formation: development, genes, and evolution** *Physiological reviews* **83**:1223–67

2. Miquerol L, Kelly RG (2013) **Organogenesis of the vertebrate heart** *Wiley Interdisciplinary Reviews: Developmental Biology* **2**:17–29

3. Leckband DE, Le Duc Q, Wang N, De Rooij J (2011) **Mechanotransduction at cadherin-mediated adhesions** *Current Opinion in Cell Biology* **23**:523–530

4. Ma L, Lu M-F, Schwartz RJ, Martin JF (2005) **Bmp2 is essential for cardiac cushion epithelial-mesenchymal transition and myocardial patterning** *Development* **132**:5601–5611

5. Rivera-Feliciano J, Tabin CJ (2006) **Bmp2 instructs cardiac progenitors to form the heart-valve-inducing field** *Developmental biology* **295**:580–588

6. Shirai M, Imanaka-Yoshida K, Schneider MD, Schwartz RJ, Morisaki T (2009) **T-box 2, a mediator of Bmp-Smad signaling, induced hyaluronan synthase 2 and Tgfbeta2 expression and endocardial cushion formation** *Proceedings of the National Academy of Sciences of the United States of America* **106**:18604–9

7. Niessen K, Fu Y, Chang L, Hoodless PA, McFadden D, Karsan A (2008) **Slug is a direct Notch target required for initiation of cardiac cushion cellularization** *Journal of Cell Biology* **182**:315–325

8. Del Monte G, Grego-Bessa J, Gonzalez-Rajal A, Bolos V, De La Pompa JL (2007) **Monitoring Notch1 activity in development: evidence for a feedback regulatory loop** *Developmental dynamics : an official publication of the American Association of Anatomists* **236**:2594–614

9. Grego-Bessa J *et al.* (2007) **Notch Signaling Is Essential for Ventricular Chamber Development** *Developmental cell* **12**:415–429

10. Timmerman LA *et al.* (2004) **Notch promotes epithelial-mesenchymal transition during cardiac development and oncogenic transformation** *Genes & development* **18**:99–115

11. Luna-Zurita L, Prados B, Grego-Bessa J, Luxan G, del Monte G, Benguria A, Adams RH, Perez-Pomares JM, de la Pompa JL (2010) **Integration of a Notch-dependent mesenchymal gene program and Bmp2-driven cell invasiveness regulates murine cardiac valve formation** *The Journal of clinical investigation* **120**:3493–507

12. Krebs LT *et al.* (2000) **Notch signaling is essential for vascular morphogenesis in mice** *Genes & development* **14**:1343–52

13. MacGrogan D *et al.* (2016) **Sequential Ligand-Dependent Notch Signaling Activation Regulates Valve Primordium Formation and Morphogenesis** *Circulation research* **118**:1480–97

14. Luxan G, D'Amato G, MacGrogan D, de la Pompa JL (2016) **Endocardial Notch Signaling in Cardiac Development and Disease** *Circulation research* **118**:e1–e18

15. Duchemin AL, Vignes H, Vermot J (2019) **Mechanically activated piezo channels modulate outflow tract valve development through the Yap1 and Klf2-Notch signaling axis** *eLife* **8**

16. Galvez-Santisteban M *et al.* (2019) **Hemodynamic-mediated endocardial signaling controls in vivo myocardial reprogramming** *eLife* **8**

17. Heckel E, Boselli F, Roth S, Krudewig A, Belting HG, Charvin G, Vermot J (2015) **Oscillatory Flow Modulates Mechanosensitive klf2a Expression through trpv4 and trpp2 during Heart Valve Development** *Current biology : CB* **25**:1354–61

18. Mounsey JP, Dimarco JP (2000) **Dofetilide** *Circulation* **102**:2665–2670

19. D'Amato G *et al.* (2016) **Sequential Notch activation regulates ventricular chamber development** *Nature cell biology* **18**:7–20

20. Joshua Lan W, Boudreau E, Stanley He D, Schachterle W, Didier Oettgen P, Brian, Benoit and Jason (2013) **ETS Factors Regulate Vegf-Dependent Arterial Specification** *Developmental cell* **26**:45–58

21. Samsa LA, Givens C, Tzima E, Stainier DY, Qian L, Liu J (2015) **Cardiac contraction activates endocardial Notch signaling to modulate chamber maturation in zebrafish** *Development* **142**:4080–91

22. Li YS, Haga JH, Chien S (2005) **Molecular basis of the effects of shear stress on vascular endothelial cells** *Journal of biomechanics* **38**:1949–71

23. Masumura T, Yamamoto K, Shimizu N, Obi S, Ando J (2009) **Shear stress increases expression of the arterial endothelial marker ephrinB2 in murine ES cells via the VEGF-Notch signaling pathways** *Arteriosclerosis, thrombosis, and vascular biology* **29**:2125–31

24. Baffi TR *et al.* (2021) **mTORC2 controls the activity of PKC and Akt by phosphorylating a conserved TOR interaction motif** *Sci Signal* **14**

25. Sarbassov DD, Ali SM, Kim DH, Guertin DA, Latek RR, Erdjument-Bromage H, Tempst P, Sabatini DM (2004) **Rictor, a novel binding partner of mTOR, defines a rapamycin-insensitive and raptor-independent pathway that regulates the cytoskeleton** *Current biology : CB* **14**:1296–302

26. Park H, Go Y-M, John PLS, Maland MC, Lisanti MP, Abrahamson DR, Jo H (1998) **Plasma Membrane Cholesterol Is a Key Molecule in Shear Stress-dependent Activation of Extracellular Signal-regulated Kinase** *Journal of Biological Chemistry* **273**:32304–32311

27. Fahie S, Cassagnol M (2023) **Verapamil StatPearls Treasure Island (FL) ineligible companies** *Disclosure: Manouchkathe Cassagnol declares no relevant financial relationships with ineligible companies* StatPearls Publishing LLC

28. Dor Y, Camenisch TD, Itin A, Fishman GI, McDonald JA, Carmeliet P, Keshet E (2001) **A novel role for VEGF in endocardial cushion formation and its potential contribution to congenital heart defects** *Development* **128**:1531–1538

29. Chang C-P, Neilson JR, Bayle JH, Gestwicki JE, Kuo A, Stankunas K, Graef IA, Crabtree GR (2004) **A Field of Myocardial-Endocardial NFAT Signaling Underlies Heart Valve Morphogenesis** *Cell* **118**:649–663

30. Fukui H, Chow RW, Xie J, Foo YY, Yap CH, Minc N, Mochizuki N, Vermot J (2021) **Bioelectric signaling and the control of cardiac cell identity in response to mechanical forces** *Science* **374**:351–354

31. Paolini A, Fontana F, Pham V-C, Rödel CJ, Abdelilah-Seyfried S (2021) **Mechanosensitive Notch-Dll4 and Klf2-Wnt9 signaling pathways intersect in guiding valvulogenesis in zebrafish** *Cell reports* **37**

32. Chow RW-Y *et al.* (2022) **Cardiac forces regulate zebrafish heart valve delamination by modulating Nfat signaling** *PLoS biology* **20**

33. Albinsson S, Nordström I, Swärd K, Hellstrand P (2008) **Differential dependence of stretch and shear stress signaling on caveolin-1 in the vascular wall** *American Journal of Physiology-Cell Physiology* **294**:C271–C279

34. Mineo C, Ying Y-S, Chapline C, Jaken S, Anderson RGW (1998) **Targeting of Protein Kinase Cα to Caveolae** *Journal of Cell Biology* **141**:601–610

35. Oka N, Yamamoto M, Schwencke C, Kawabe J-I, Ebina T, Ohno S, Couet J, Lisanti MP, Ishikawa Y (1997) **Caveolin Interaction with Protein Kinase C** *Journal of Biological Chemistry* **272**:33416–33421

36. Sural-Fehr T, Singh H, Cantuti-Catelvetri L, Zhu H, Marshall MS, Rebiai R, Jastrzebski MJ, Givogri MI, Rasenick MM, Bongarzone ER (2019) **Inhibition of IGF-1-PI3K-Akt-mTORC2 in lipid rafts increases neuronal vulnerability in a genetic lysosomal glycosphingolipidosis** *Disease models & mechanisms* **12**

37. White AB, Givogri MI, Lopez-Rosas A, Cao H, Van Breemen R, Thinakaran G, Bongarzone ER (2009) **Psychosine Accumulates in Membrane Microdomains in the Brain of Krabbe Patients, Disrupting the Raft Architecture** *The Journal of Neuroscience* **29**:6068–6077

38. Yamamoto K, Ando J (2013) **Endothelial cell and model membranes respond to shear stress by rapidly decreasing the order of their lipid phases** *Journal of cell science* **126**:1227–1234

39. Steinbuck MP, Arakcheeva K, Winandy S (2018) **Novel TCR-Mediated Mechanisms of Notch Activation and Signaling** *The Journal of Immunology* **200**:997–1007

40. Goenezen S, Rennie MY, Rugonyi S (2012) **Biomechanics of early cardiac development** *Biomechanics and modeling in mechanobiology* **11**:1187–204

41. Doubilet PM, Benson CB, Chow JS (1999) **Long-term prognosis of pregnancies complicated by slow embryonic heart rates in the early first trimester** *Journal of Ultrasound in Medicine* **18**:537–541

42. Braga M, Moleiro ML, Guedes-Martins L (2019) **Clinical Significance of Ductus Venosus Waveform as Generated by Pressure-volume Changes in the Fetal Heart** *Curr Cardiol Rev* **15**:167–176

Author information

Yunfei Mu[#]
Fudan University, Shanghai, China, Key Laboratory of Growth Regulation and Translational Research of Zhejiang Province, School of Life Sciences, Westlake University, Hangzhou, China, Westlake Laboratory of Life Sciences and Biomedicine, Hangzhou, China, Institute of Basic Medical Sciences, Westlake Institute for Advanced Study, Hangzhou, China

[#]These authors contributed equally to this article.

Shijia Hu[#]
Fudan University, Shanghai, China, Key Laboratory of Growth Regulation and Translational Research of Zhejiang Province, School of Life Sciences, Westlake University, Hangzhou, China, Westlake Laboratory of Life Sciences and Biomedicine, Hangzhou, China, Institute of Basic Medical Sciences, Westlake Institute for Advanced Study, Hangzhou, China

[#]These authors contributed equally to this article.

Xiangyang Liu
Key Laboratory of Growth Regulation and Translational Research of Zhejiang Province, School of Life Sciences, Westlake University, Hangzhou, China, Westlake Laboratory of Life Sciences and Biomedicine, Hangzhou, China, Institute of Basic Medical Sciences, Westlake Institute for Advanced Study, Hangzhou, China

Xin Tang
Key Laboratory of Growth Regulation and Translational Research of Zhejiang Province, School of Life Sciences, Westlake University, Hangzhou, China, Westlake Laboratory of Life Sciences and Biomedicine, Hangzhou, China, Institute of Basic Medical Sciences, Westlake Institute for Advanced Study, Hangzhou, China

Jiayi Lin
Key Laboratory of Growth Regulation and Translational Research of Zhejiang Province, School of Life Sciences, Westlake University, Hangzhou, China, Westlake Laboratory of Life Sciences and Biomedicine, Hangzhou, China, Institute of Basic Medical Sciences, Westlake Institute for Advanced Study, Hangzhou, China

Hongjun Shi
Key Laboratory of Growth Regulation and Translational Research of Zhejiang Province, School of Life Sciences, Westlake University, Hangzhou, China, Westlake Laboratory of Life Sciences and Biomedicine, Hangzhou, China, Institute of Basic Medical Sciences, Westlake Institute for Advanced Study, Hangzhou, China
ORCID iD: 0000-0002-4993-2322

For correspondence: shihongjun@westlake.edu.cn

Editors

Reviewing Editor
Caroline Burns
Boston Children's Hospital, Boston, United States of America

Senior Editor
Kathryn Cheah
University of Hong Kong, Hong Kong, Hong Kong

Reviewer #2 (Public review):

Summary:

In mice, Notch1 is expressed uniformly throughout the endocardium during the initial stages of heart valve formation. How, then, is Notch activated specifically in the valve forming regions? To answer this question, the authors use a combination of in vivo and ex vivo experiments to demonstrate the critical role of hemodynamic forces on Notch1 activation and provide strong evidence for a novel mechanotransduction pathway involving PKC and mTORC2.

Strengths:

(1) Novel insights into the role of PKC and mTOR were obtained using a combination of mutant studies and pharmacological studies.
(2) Novel insights on the role of mechanical forces on caveolin-1 localisation.
(3) Mechanical forces were manipulated using the class III antiarrhythmic drug dofetilide, which transiently blocks heartbeat. Care was taken to minimise the confounding effects of hypoxia.

Weaknesses:

The authors suggest that shear stress activates the mTORC2-PKC-Notch signalling pathway by altering the membrane lipid microstructure. Although this is a fascinating hypothesis, more evidence will be needed to prove this. In particular, it is not clear how the general addition of cholesterol in dofetilide-treated hearts would result in a rescue of regionalized membrane distribution within the AVC and in high-shear stress areas.

https://doi.org/10.7554/eLife.97268.2.sa2

Reviewer #3 (Public review):

Summary:

The overall goal of this manuscript is to understand how Notch signaling is activated in specific regions of the endocardium, including the OFT and AVC, that undergo EMT to form the endocardial cushions. Using dofetilide to transiently block circulation in E9.5 mice, the authors show that Notch receptor cleavage still occurs in the valve-forming regions due to mechanical sheer stress as Notch ligand expression and oxygen levels are unaffected. The authors go on to show that changes in lipid membrane structure activate mTOR signaling, which causes phosphorylation of PKC and Notch receptor cleavage. The data are largely convincing and support their hypothesis. The conclusions are also novel and significantly add to the field of endocardial cushion biology.

The strengths of the manuscript include the dual pharmacological and genetic approaches to block blood flow in the mouse, the inclusion of many controls including those for hypoxia, the quality of the imaging, and the clarity of the text. In the revision, the authors put forth a good faith effort to address experimentally or textually the concerns of the reviewers. Most weaknesses that were identified in the first submission were addressed and the main claims are convincing. In general, the authors achieved their aims and the results support their conclusions.

https://doi.org/10.7554/eLife.97268.2.sa1

Author response:

The following is the authors' response to the original reviews.

> ***Public Review:***
>
> *The overall goal of this manuscript is to understand how Notch signaling is activated in specific regions of the endocardium, including the OFT and AVC, that undergo EMT to form the endocardial cushions. Using dofetilide to transiently block circulation in E9.5 mice, the authors show that Notch receptor cleavage still occurs in the valve-forming regions due to mechanical sheer stress as Notch ligand expression and oxygen levels are unaffected. The authors go on to show that changes in lipid membrane structure activate mTOR signaling, which causes phosphorylation of PKC and Notch receptor cleavage.*
>
> *The strengths of the manuscript include the dual pharmacological and genetic approaches to block blood flow in the mouse, the inclusion of many controls including those for hypoxia, the quality of the imaging, and the clarity of the text. However, several weaknesses were noted surrounding the main claims where the supporting data are incomplete.*
>
> *PKC - Notch1 activation:*
>
> *(1) Does deletion of Prkce and Prkch affect blood flow, and if so, might that be suppressing Notch1 activation indirectly?*

To address this concern, we performed echocardiography of *Prkce*$^{+/-}$;*Prkch*$^{+/-}$, *Prkce*$^{-/-}$;*Prkch*$^{+/-}$, and *Prkce*$^{+/-}$;*Prkch*$^{-/-}$ mouse hearts (Figure 3-supplement figure 2D), showing no significant effect in heartbeat and blood flow. (Line 308)

> *(2) It would be helpful to visualize the expression of prkce and prkch by in situ hybridization in E9.5 embryos.*

We now added immunofluorescence staining results for both PKCE and PKCH as shown in Figure 3-supplement figure 2B. In E9.5 embryonic heart, PKCH is mainly expressed in the endocardium overlying AV canal and the base of trabeculae, overlapping with the expression pattern of NICD and pPKC^{Ser660}. PKCE is expressed in both endocardium and myocardium. In the endocardium, PKCE is mainly expressed in the endocardium overlying AV canal (Line312-314)

> *(2) PMA experiments: Line 223-224: A major concern is related to the conclusion that "blood flow activates Notch in the cushion endocardium via the mTORC2-PKC signaling pathway". To make that claim, the authors show that a pharmacological activation with a potent PKC activator, PMA, rescues NICD levels in the AVC in dofetilide-treated embryos. This claim would also need proof that a lack of blood flow alters the activity of mTORC2 to phosphorylate the targets of PKC phosphorylation. Also, this observation does not explain the link between PKC activity and Notch activation.*

Both AKT Ser473 and PKC Ser660 are well characterized phosphorylation sites regulated by mTORC2 (Baffi TR et. al, mTORC2 controls the activity of PKC and Akt by phosphorylating a conserved TOR interaction motif. Sci Signal. 2021;14.). pAKT^{Ser473} is widely used as an indicator of mTORC2 activity. Therefore, the reduced staining intensity of pAKT^{Ser473} and pPKC^{Ser660} observed in the dofetilide treated embryos should reflect the reduced activity of their common upstream activator mTORC2. This information is provided in Line 317-321.

As PMA is a well-characterized specific activator of PKC, we believe the rescue of NICD by PMA could explain the link between PKC activity and Notch activation.

> *(3) In addition, the authors hypothesise that shear stress lies upstream of PKC and Notch activation, and that because shear stress is highest at the valve-forming regions, PKC and Notch activity is localised to the valve-forming regions. Since PMA treatment affects the entire endocardium which expresses Notch1, NICD should be seen in areas outside of the AVC in the PMA+dofetilide condition. Please clarify.*

As shown in Figure 3C and Figure 3-supplement figure 2B, pPKC, PKCH and PKCE expression are all confined in the AVC region. This explains PMA activates NICD specifically in the valve-forming region. This information is added in Line 312-314.

> *Lipid Membrane:*
>
> *(1) It is not clear how the authors think that the addition of cholesterol changes the lipid membrane structure or alters Cav-1 distribution. Can this be addressed? Does adding cholesterol make the membrane more stiff? Does increased stiffness result from higher shear stress?*

We do not know how exactly addition of cholesterol alters membrane structure and influence mTORC2-PKC-Notch signaling. As cholesterol is an important component of lipid raft and caveolae, it is possible that enrichment of cholesterol might alter the membrane structure to make the lipid raft structure less dependent on sheer stress. This hypothesis need to be tested in further in vitro studies. This information is added to Line 433-436.

> *(2) The loss of blood flow apparently affects Cav1 membrane localization and causes a redistribution from the luminal compartment to lateral cell adhesion sites. Cholesterol treatment of dofetilide-treated hearts (lacking blood flow) rescued Cav1 localization to luminal membrane microdomains and rescued NICD expression. It remains unclear how the general addition of cholesterol would result in a rescue of regionalized membrane distribution within the AVC and in high-shear stress areas.*

We do not know the exact mechanism. As replied in the previous question, future cell-based work is needed to address these important questions. (Line 433-436)

> *(3) The authors do not show the entire heart in that rescue treatment condition (cholesterol in dofetilide-treated hearts). Also, there is no quantification of that rescue in Figure 4B. Currently, only overview images of the heart are shown but high-resolution images on a subcellular scale (such as electron microscopy) are needed to resolve and show membrane microdomains of caveolae with Cav1 distribution. This is important because Cav-1could have functions independent of caveolae.*

In Figure 4C, most panels display the large part of the heart including AVC, atrium and ventricle. The images in the third column appear to be more restricted to AVC. We have now replaced these images to reveal AVC and part of the atrium and ventricle.

The quantification has also been provided in Figure 4C. We also added a new panel of scanning EM of AVC endocardium, showing numerous membrane invaginations on the luminal surface of the endocardial cells. The size of the invaginations ranges from 50 to 100 nm, consistent with the reported size of caveolae. Dofetilide significantly reduced the number of membrane invaginations, which recovered after restore of blood flow at 5 hours post dofetilide treatment. The reduction of membrane invaginations could also be rescued by ex vivo cholesterol treatment. This information is added to Line 342-349.

> *Figure Legends, missing data, and clarity:*
>
> *(1) The number of embryos used in each experiment is not clear in the text or figure legends. In general, figure legends are incomplete (for instance in Figure 1).*

Thanks for reminding. we have now added numbers of embryos in the figure legends.

> *(2) Line 204: The authors refer to unpublished endocardial RNAseq data from E9.5 embryos. These data must be provided with this manuscript if it is referred to in any way in the text.*

The RNAseq data of PKC isoforms is now provided in Figure3-Figure supplement 2A, Line 301-302.

> *(3) Figure 1 shows Dll4 transcript levels, which do not necessarily correlate with protein levels. It would be important to show quantifications of these patterns as Notch/Dll4 levels are cycling and may vary with time and between different hearts.*

The Dll4 immuno-staining in Figure 1B,C is indeed Dll4 protein, not transcript. The quantification is added in Figure 1—Figure supplement 1C. Line 215.

> *(4) Line 212-214: The authors describe cardiac cushion defects due to the loss of blood flow and refer to some quantifications that are not completely shown in Figure 3. For instance, quantifications for cushion cellularity and cardiac defects at three hours (after the start of treatment?) are missing.*

The formation of the defects is a developmental process and time dependent. To address this concern, we quantified the cushion cellularity at 5 hours post dofetilide treatment and showed that cell density significantly decreased in the dofetilide treated embryos, albeit less pronounced than the difference at E10.5. (Line 256-257)

> *(5) Related to Figure 5. The work would be strengthened by quantification of the effects of dofetilide and verapamil on heartbeat at the doses applied. Is the verapamil dosage used here similar to the dose used in the clinic?*

We are grateful to this suggestion. The effect of dofetilide on heartbeat has already been shown in Figure 2A. We have now additionally measured the heartbeat rate of verapamil treated embryos, and provided the results in Figure 5E. For verapamil injection in mice, a single i.p. dose of 15 mg/kg was used, which is equivalent to 53 mg/m^2 body surface. Verapamil is used in the clinic at dosage ranging from 200 to 480 mg/day, equivalent to 3.33 - 8 mg/kg or 117 - 282 mg/m^2 body surface. Therefore, the dosage used in the mouse is not excessively high compared to the clinic uses. (Line 361-365)

> *Overstated Claims:*
>
> *(1) The authors claim that the lipid microstructure/mTORC2/PKC/Notch pathway is responsive to shear stress, rather than other mechanical forces or myocardial function. Their conclusions seem to be extrapolated from various in vitro studies using non-endocardial cells. To solidify this claim, the authors would need additional biomechanical data, which could be obtained via theoretical modelling or using mouse heart valve explants. This issue could also be addressed by the authors simply softening their conclusions.*

We aggrege with the reviewer's comment. We have now revised the statement as "Our data support a model that membrane lipid microdomain acts as a shear stress sensor and transduces the mechanical cue to activate intracellular mTORC2-PKC-Notch signaling pathway in the developing endocardium. (line 416-418) It is noteworthy that the methodology used to alter blood flow in this study inevitably affects myocardial contraction. Additional work to uncouple sheer stress with other changes of mechanical properties of the myocardium with the aid of theoretical modelling or using mouse heart valve explants is needed to fully characterize the effect of sheer stress on mouse endocardial development." (Line 436-440)

> *(2) Line 263-264: In the discussion, the authors conclude that "Strong fluid shear stress in the AVC and OFT promotes the formation of caveolae on the luminal surface of the endocardial cells, which enhances PKCε phosphorylation by mTORC2." This link was shown rather indirectly, rather than by direct evidence, and therefore the conclusion should be softened. For example, the authors could state that their data are consistent with this model.*

We have revised the statement as "Strong fluid shear stress in the AVC and OFT enhances PKC phosphorylation by mTORC2 possibly by maintaining a particular membrane microstructure." (Line 372-374)

> *(3) In the Discussion, it says: "Mammalian embryonic endocardium undergoes extensive EMT to form valve primordia while zebrafish valves are primarily the product of endocardial infolding (Duchemin et al., 2019)." In the paper cited, Duchemin and colleagues described the formation of the zebrafish outflow tract valve. The zebrafish atrioventricular valve primordia is formed via partial EMT through Dll-Notch signaling (Paolini et al. Cell Reports 2021) and the collective cell migration of endocardial cells into the cardiac jelly. Then, a small subset of cells that have migrated into the cardiac jelly give rise to the valve interstitial cells, while the remainder undergo mesenchymal-to-endothelial transition and become endothelial cells that line the sinus of the atrioventricular valve (Chow et al., doi: 10.1371/journal.pbio.3001505). The authors should modify this part of the Discussion and cite the relevant zebrafish literature.*

Thanks for valuable comments. We have now revised the statement as "Mammalian embryonic endocardium undergoes extensive EMT to form valve primordia while zebrafish atrioventricular valve primordia is formed via partial EMT and the collective cell migration of endocardial cells into the cardiac jelly followed by tissue sheet delamination." with relevant references added. (Line 411-414)

> ***Recommendations to the Authors:***
>
> *(1) One issue that the authors could address is the organization of figures. There are several cases where positive data that are central to the conclusions are placed in the supplement and should be moved to the main figures. Places where this occurred are listed below:*
>
> *- The Tie2 conditional deletion of Dll4 showing retention of NICD in the OFT and AVC regions is highly supportive of the model. The authors should consider moving these data to main Figure 1.*

Thanks for the suggestion. We have reorganized the figure as requested.

> *- The ligand expression data in Figure 2- Supplement Figure 1 A is VERY important to the conclusions drawn from the dofetilide treatment. The authors should move these data to*

> *main Figure 2.*

The ligand expression data in Figure 2- Supplement Figure 1A are now moved to Figure 2B.

> *- In Figure 3A - the area in the field of view should be stated in the Figure (is it the AVC?) Figure 3 - Supplement 1 proximal OFT data should be moved to main Figure 3 as it is central to the conclusions. Negative DA data can be left in the supplement. Again, for Figure 3 - Supplement 1 Stauroporine treatment data should be moved to the main figure as it is positive data that are central to the conclusions.*

Thanks for the suggestion. We have reorganized the figure as requested.

> *(2) Antibody used for Twist1 detection is not listed in the resource table.*

Twist1 is purchased from abcam, the detailed information is now available in the resource table.

> *(3) Missing arrowhead in Figure 4A, last row.*

Sorry for the negligence. Arrowhead is now added.

> *(4) Line 286. "OFT" pasted on the word "endothelium".*

“OFT” is now removed.

> *(5) Related to Figure 2C. The fast response of NICD to flow cessation was used as an argument to support post-translational modification. It is not clear why Sox9 and Twist1 expression also responds so quickly.*

Sox9 and Twist1 expression does seem to respond very quickly. Whether there exists additional regulatory pathways such as Wnt, Vegf signaling that also respond to sheer stress needs to be investigated in the future.

> *(6) Line 200: The sentence should end with a period.*

Sorry for the oversight. It is now corrected.

> *(7) Lines 34 to 35: the authors phrase that Notch is "allowed" to be specifically activated in the AVC and outflow tract by shear stress.*

We have rephrased the statement with “enabling Notch to be specifically activated in AVC and OFT by regional increased shear stress.” Line 27

> *(8) Lines 96-100: At the end of the introduction, the text is copied from the abstract. New text should be written or summarized in a different way.*

The last sentence of introduction is now changed to “The results uncovered a new mechanism whereby mechanical force serves as a primary cue for endocardial patterning in mammalian embryonic heart.” (Line 93-95)

> *(9) Line 125: The term "agreed with the Dll4 transcript.."should be replaced with a better term like "overlapped" or "was identical with".*

The word “agreed” is now “overlapped”. (Line 219)

> *(10) Line 291: "Thus, through these sophisticated mechanisms, the developing mouse hearts may achieve three purposes:"- The English should be adjusted here since it sounds like hearts are aiming to achieve a purpose, which is unlikely what was meant by the authors.*

This sentence is rephrased to “Thus, in the developing mouse hearts: (1) VEGF signaling is reduced to permit endocardial EMT; (2) Dll4 expression is reduced to prevent widespread endocardial Notch activation and make endocardium sensitive to flow; (3) a proper cushion size and shape is maintained by limiting the flanking endocardium to undergo EMT despite physically close to the field of BMP2 derived from of AVC myocardium (Figure 6).” (Line 402-406)

https://doi.org/10.7554/eLife.97268.2.sa0